



Designing Multirate Control for a Robotic Manipulator in the Presence of Disturbance

Hossein Ghasemzadeh Ebli ¹, Mohammad Ali Nekoui ^{2*}, Mohammad Teshnelab ²

¹ Department of Electrical Engineering, Islamic Azad University, South Tehran Branch., Tehran, Iran

² Department of Electrical Engineering, K. N. Toosi University of Technology, Tehran, Iran

Corresponding author; manekoui@kntu.ac.ir

Abstract

In the present paper, multirate control method is used for mechanical robotic manipulators. Also, the process of designing the reference state vector for mechanical manipulators is presented in this paper. For this purpose, a prototype robot is assumed in which highly precise rotary encoders are mounted at the outer side of the joints. The robot dynamics is time-continuous while the relevant controls are time-discrete. Since these systems are always exposed to unwanted disturbances, the present paper introduces a passivity-based control that, in contrast to the reverse dynamic controls, doesn't require linearization. In this regard, first, the modified form of the Lyapunov-based control and, then, the discretized equations are presented. The multirate controller is implemented on the discretized structure and, thereby, its effect on the estimation precision of the angles of the joints is examined in comparison with the single-rate controls. In the method presented in this paper, a multi-rate controller can lead to an accurate routing with the least detail of the nonlinear dynamics of the robot. The main goal is to improve the accuracy of the manipulator robot's ability to track reference input under the influence of fixed finite disturbances. The simulation results performed on the manipulator prove that under appropriate assumptions, accurate path tracking and input disturbance rejection can be achieved using the proposed structure.

Keywords: Multirate control, Robotic Manipulator, Network Control System, Disturbances, Lyapunov based Control

Article history: Submitted 21-May-2022; Revised 02-Jun-2022; Accepted 12-Jun-2022. Article Type: Research paper

© 2023 IAUCTB-IJSEE Science. All rights reserved

<https://doi.org/10.30495/ijsee.2022.1959264.1203>

1. Introduction

The idea of resource allocation in network systems was first presented in [1] aiming to investigate the stability of the network systems with a high volume of data. This method was then generalized in [2]-[9]. Another common problem in network systems is the quantization error. This problem was studied in [6]-[7]. The method of sampling the output continuous signal of the systems in network structures is one of the important issues in the field of system stability. In [8]-[9], a network structure, consisting of a sampler linear system and an unknown time-varying delay, has been discussed. Nevertheless, the two major disadvantages of this system are that the sampling intervals are assumed constant and monotonous and the delay is upper-bounded so that the upper bound is a function of the

sampling time. The more general form of these network structures has been studied in [10]-[15]. In these articles, the delay has been assumed as time-varying and unknown and the sampling rate has been considered non-monotonous. Besides, sufficient conditions have been taken into consideration for stability.

An obstacle to the improvement of the robotic manipulators performance is the residual vibration resulting from the weakness of the reducing gears mounted on the joints of the mechanical manipulators. Some articles have introduced mathematical models that modeled features of the reducing gears. In particular, Kuslaka & Shimada [16] described a controller design technique that exploited features of the reducing gears. By

considering the presentation of the state space for the disturbance observer, this technique improved the controller's performance. This technique not only considered the error between the reference rotor angles and the actual rotor angles but also reduced the error between the joint's angles. Despite its successful performance in reducing the residual vibrations, this technique failed to exhibit a good routing or tracking performance. Of course, this problem has been solved in the present work. The main idea of this paper is to use multirate control and consider sampling time as one of the control parameters, as a consequence of which this time can be determined by the designer and can be increased or decreased depending on the robot's motion path.

In Reference [17] provides a multi-rate controller for critical safety systems in that a high-level programmer and a low-level controller are assumed to be able to operate at different frequencies. This multi-rate controller is simulated by a one-line nonlinear model that evolves on a continuous and discrete level. A method for the stability of the multi-rate controller for linear systems with single perturbation is to use the proposed multi-rate sampling data control rule based on the multi-rate discretization method on the continuous-time combined control law, which is derived from the single perturbation theory. In this method, sampling times should be asynchronous and non-uniformly spaced, although the variables are slow and fast. In this reference [18] a time-dependent Lyapunov function is introduced to analyse the closed-loop stability of a system intended with multi-rate feedback.

One of the most widely used systems in the production process is the sample data control industry. Recently, multi-rate sampling has attracted much attention in the study of sampling data control theory. If the sampling periods for the state variables are different from the system input periods, under these conditions we will be able to design an equivalent discrete time system using the lift technique. In this reference [19] a new algorithm is proposed using matrix alternatives to solve the control problem of linear quadratic regulator (LQR) of multi-rate systems. Thus, using the least squares method, the out-of-policy algorithm becomes a modelless reinforcement learning algorithm that requires only system input and output data.

In the method presented in this paper, a multi-rate controller can lead to an accurate routing with the least detail of the nonlinear dynamics of the robot. The main goal is to improve the accuracy of the manipulator robot's ability to track reference input under the influence of fixed finite disturbances. The simulation results performed on the manipulator prove that under appropriate

assumptions, accurate path tracking and input disturbance rejection can be achieved using the proposed structure.

The position and velocity estimation method using the Adaptive Kalman Filter (AREKF). The motion and velocity of each joint are predicted for use in the Lyapunov-based discontinuous control structure for robotic manipulators subjected to fixed boundary disturbances [20].

Considering the above-mentioned introduction, the rest of the present paper is organized as follows. Section 2 presents the dynamics of the robot in both workspace and joint space along with the relevant equations. In Section 3, the Lyapunov-based controller and its modified discrete structure are introduced. Section 4 includes designing a multirate control. The simulation results are presented in Section 5. And finally, Section 6 is allocated to the conclusion

2. Robotic Manipulator System Modeling

To extract dynamic equations of robots based on the Lagrangian method, the first step is to form the Lagrangian. The Lagrangian is defined as the difference between the kinetic and potential energies of the robot [20]:

$$L = K - P \quad (1)$$

where K is the sum of all kinetic energy terms and P is the sum of all potential energy terms of the system. Let's assume that $q = (q_1 \ \dots \ q_n)^T$ and $\dot{q} = (\dot{q}_1 \ \dots \ \dot{q}_n)^T$ are the generalized coordinates vector and generalized velocities vector, respectively. Also, assume that τ_i is the force generalized at the i^{th} joint meaning that this term represents the torque for the rotary joint and force for the telescopic joint. On this basis, the Lagrangian equation is expressed as follows:

$$\frac{d}{dt} \left(\frac{\partial L}{\partial \dot{q}_i} \right) - \frac{\partial L}{\partial q_i} = \tau_i \quad i = 1, 2, \dots, n \quad (2)$$

The kinetic energy of a rigid object can be obtained using the following equation:

$$K = \frac{1}{2} m v^T v + \frac{1}{2} \omega^T \Gamma \omega \quad (3)$$

Where m is the total mass of the object, v is the linear velocity, ω is the angular velocity, and Γ is the symmetric 3×3 matrix called inertia matrix.

Apropos of the above kinetic energy, it is evident that the linear and angular velocities v and ω have been expressed within the inert framework. Now, we assume that I and Γ indicate the inertia matrix relative to the object-connected frame and the

earth frame (inert frame), respectively. Evidently, I is not dependent on the rotation of the object but we have:

$$\Gamma = RIR^T \quad (4)$$

Now, let's assume a robot with n links. By converting the above set of equations into the matrix form, we will have:

$$M(q)\ddot{q} + C(q, \dot{q})\dot{q} + G(q) = \tau \quad (5)$$

In this form, M is the inertia matrix of mass and, C is the Coriolis matrix, G is the Gravity vector, and τ is the vector of joint torques.

It should be noted that vector G includes the system's potential energy gradient terms.

The state equation will be as follows:

$$\dot{x} = f(x) + g(x)u = f(x) + \sum_{j=1}^n g_j(x)u_j \quad (6)$$

where

$$f(x) = \begin{bmatrix} q \\ -M^{-1}(q)\{(C(q, \dot{q}))\dot{q} + G(q)\} \end{bmatrix} \quad (7)$$

$$g(x) = \begin{bmatrix} 0_{n \times n} \\ M^{-1}(q) \end{bmatrix} u = f(x) + g(x)u$$

3. Controller used for elimination of Disturbance

The main idea is to find a nonlinear feedback control rule to eliminate the effects of all nonlinear factors so that the closed-loop dynamic equation of the system becomes a linear form. Using this controller, we try to eliminate the effects of constant and limited disturbance on the robot.

This controller is indeed a kind of passivity-based controller that, unlike reverse dynamic controllers, doesn't require linearization. For this purpose, first, we assume the following variables:

$$\begin{cases} \dot{\xi} = \dot{q}_d - F(\circ)\tilde{q} \\ \sigma = \dot{q} - \dot{\xi} \end{cases} \quad (8)$$

$$\rightarrow \sigma = \dot{q} + F(\circ)\tilde{q} \xrightarrow{\text{Laplace}} \sigma(s) = (sI + F(s))\tilde{q}(s)$$

$F(0)$ can be assumed as any linear operator, in the condition that mapping $H(s) = (sI + F(s))^{-1}$ be strictly proper and stable. $H(s)$ is applied as an operator to map trajectory tracking error to a new variable σ . Based on this substitution, the Lyapunov-based controller law can be derived as:

$$u := D(q)\ddot{\xi} + C(q, \dot{q})\xi + G(q) - K_D\sigma - \hat{d} \quad (9)$$

Where K_D is a positive definite symmetric matrix, \hat{d} is an estimation of d . We assume that $\tilde{d} = d - \hat{d}$, which can be considered as the estimation error. We have:

$$D(q)\dot{\sigma} + C(q, \dot{q})\sigma + K_D\sigma = \tilde{d} \quad (10)$$

Using the passivity theorem, if \tilde{d} is bounded and mapping of $-\sigma \mapsto \tilde{d}$ is passive relative to function of $V1$, then $\tilde{q}, \dot{\tilde{q}}$ will be continuous and $\tilde{q}, \dot{\tilde{q}}$ will asymptotically converge to zero. This fact can be presented by:

$$\lim_{t \rightarrow \infty} \tilde{q}(t) = \lim_{t \rightarrow \infty} \dot{\tilde{q}}(t) = 0 \quad (11)$$

We assume the Lyapunov function as follows:

$$V := \frac{1}{2}\sigma^T D(q)\sigma + \frac{1}{2}\tilde{d}^T K_I^{-1}\tilde{d} \quad (12)$$

Now, the derivative of the Lyapunov function can be calculated as follows:

$$\begin{aligned} \dot{V} &= \sigma^T D(q)\dot{\sigma} + \frac{1}{2}\sigma^T \dot{D}(q)\sigma + \tilde{d}^T K_I^{-1}\dot{\tilde{d}} \\ &= \sigma^T (-C(q, \dot{q})\sigma - K_D\sigma + \tilde{d}) + \frac{1}{2}\sigma^T \dot{D}(q)\sigma + \tilde{d}^T K_I^{-1}\dot{\tilde{d}} \\ &= \frac{1}{2}\sigma^T (\dot{D}(q) - 2C(q, \dot{q}))\sigma - \sigma^T K_D\sigma + \tilde{d}^T (\sigma + K_I^{-1}\dot{\tilde{d}}) \\ &= -\sigma^T K_D\sigma + \tilde{d}^T (\sigma + K_I^{-1}\dot{\tilde{d}}) \end{aligned} \quad (13)$$

The derivative of error estimation is:

$$\sigma + K_I^{-1}\dot{\tilde{d}} = 0 \rightarrow \dot{\tilde{d}} = -K_I\sigma \quad (14)$$

We have:

$$\dot{V} = -\sigma^T K_D\sigma \leq 0 \quad (15)$$

Now, using the following inequality:

$$V(t) - V(0) \leq -\lambda_{\min}(K_D) \int_0^t \|\sigma(s)\|^2 ds \quad (16)$$

We can conclude that $\sigma \in L_2$. So, we can write:

$$\begin{aligned} \dot{\sigma} &\in L_\infty \\ \dot{V} &= -\sigma^T K_D\sigma \rightarrow \ddot{V} = -2\sigma^T K_D\dot{\sigma} \end{aligned} \quad (17)$$

$$\sigma, \dot{\sigma} \in L_\infty \rightarrow \ddot{V} \in L_\infty$$

Using Barbalat's lemma, we can show that:

$$\dot{V} \in L_\infty \quad (18)$$

And

$$\lim_{t \rightarrow \infty} V(t) < \infty \quad (19)$$

So, we have

$$\lim_{t \rightarrow \infty} \dot{V}(t) = 0 \rightarrow \lim_{t \rightarrow \infty} \sigma = 0 \quad (20)$$

So, the parameter update law is changed into the following form:

$$\begin{aligned}
-\sigma^T \tilde{d} &= -\dot{d}^T K_I^{-1} \tilde{d} = \dot{d}^T K_I^{-1} \tilde{d} \\
\int_0^t -\sigma^T(s) \tilde{d}(s) ds &= \int_0^t \dot{d}^T(s) K_I^{-1} \tilde{d}(s) ds = \frac{1}{2} \dot{d}^T K_I^{-1} \tilde{d} \Big|_0^t \quad (21) \\
&= \frac{1}{2} \dot{d}^T K_I^{-1} \tilde{d} - \frac{1}{2} \dot{d}^T(0) K_I^{-1} \tilde{d}(0) \\
&= V_1(t) - V_1(0)
\end{aligned}$$

where

$$V_1 = \frac{1}{2} \dot{d}^T K_I^{-1} \tilde{d} \quad (22)$$

Eventually, the final form of this controller can be expressed as follows:

$$u = D(q)\ddot{\zeta} + C(q, \dot{q})\dot{\zeta} + G(q) - K_D\sigma - K_I \int_0^t \sigma(s) ds \quad (23)$$

4. Designing a Multirate Feed forward Controller

Assume bellow that (A_c, B_c) is controllable and defining matrix, $B_c = [b_1, b_2, \dots, b_m]$ in continue the following matrix is obtained:

$$\begin{aligned}
H &= [b_1, A_c b_1, \dots, A_c^{n_1-1} b_1, A_c b_2, \dots, A_c^{n_2-1} b_2 \\
&\dots, b_m, A_c b_m, \dots, A_c^{n_m-1} b_m] \quad (24)
\end{aligned}$$

Where the components must be chosen in such a way that $n_1 = n_2 = \dots = n_m = n/m$. By using the vector of the $\zeta_i = n_1 + n_2 + \dots + n_i$ row of the matrix H^{-1} , the following matrix is obtained:

$$\begin{aligned}
S &= [h_1, A_c h_1, \dots, A_c^{n_1-1} h_1, \dots, h_m, A_c h_m, \\
&\dots, A_c^{n_m-1} h_m]^T \quad (25)
\end{aligned}$$

In addition, the transformation of coordinates is done for S using $z = S \cdot x_c$. Then, the resulting system, which is shown below:

$$\{A, B, C, 0\} = \{SA_c S^{-1}, SB_c, C_c S^{-1}, 0\} \quad (26)$$

That expressed in a controllable standard form. Finally, by discretizing the system, the state variables are expressed using digital data. In this paper, this process is performed using (m=2, n=8).

The mathematical model of the mechanical manipulator is written in such a way that the multirate control law for the mechanical manipulator can be implemented on it. For the mechanical manipulator, which has m input and m outputs and is of the order of n the input controller updates the control and tracks the output N times, which is equal to the update ratio of T_t based on its

position. Also, in this control, the utility functions are as $T_s = T_t/N$ and $N = n/m$ so that N is a natural number.

$$\dot{x} = A_c x(t) + B_c u(t), y(t) = C_c x(t) \quad (27)$$

The mechanical manipulator model is

discretized by the control ratio of T_s and expressed as follows:

$$P(z_s) = [A_s, B_s, C_s, D_s] \quad (28)$$

And

$$x(i, j) := x[(i + j/N) T_l] \quad (29)$$

Therefore, the results of Equations (30) and (31) can be obtained in which $0 \leq j < N$ and (i, j)

represent the time of, $t = (i + j/N) T_r$.

$$x_s(i, j + 1) = A_s x_s(i, j) + B_s u(i, j) \quad (30)$$

$$y(i, j) = C_s x_s(i, j) + D_s u(i, j) \quad (31)$$

Where

$$A_s = e^{A_c T_s}, B_s = \int_0^{T_s} e^{A_c \tau} B_c d\tau, C_s = C_c \quad (32)$$

The feedback control is designed using the above equations. In practice, when updating occurs N times, the discrete model

$$P(z_l) = [A_l, B_l, C_l, D_l] \quad (33)$$

With a control ratio of T_l is obtained.

Whenever $x_l(i) = x_l[iT_l]$ indicates the state variable, then

$$u(i) = [u(i, 1), \dots, u(i, N)]^T \quad (34)$$

And

$$y(i) = [y(i, 1), \dots, y(i, N)]^T \quad (35)$$

Indicate the input vector and output vector of the control. By using these parameters, Equations (36) and (37) can be obtained.

$$x_l(i + 1) = A_l x_l(i) + B_l u(i) \quad (36)$$

$$y(i) = C_l x_l(i) + D_l u(i) \quad (37)$$

Where

$$\begin{bmatrix} A_l & B_l \\ C_l & D_l \end{bmatrix} := \begin{bmatrix} e^{A_c T_r} & B_1 & \dots & B_N \\ C_1 & D_{11} & \dots & D_{1N} \\ \vdots & \vdots & \ddots & \vdots \\ C_N & D_{N1} & \dots & D_{NN} \end{bmatrix}$$

$$B_j := \int_{(1-\mu_j)T_r}^{(1-\mu_{j-1})T_r} e^{A_c \tau} B_c d\tau$$

$$C_k := C_c e^{A_c v_k T_r}$$

$$D_{kj} := \mu_j < v_k : C_c \int_{(v_k - \mu_j)T_r}^{(v_k - \mu_{j-1})T_r} e^{A_c \tau} B_c d\tau$$

$$\begin{aligned} \mu_{(j-1)} < v_k \leq \mu_j : C_c \int_0^{(v_k - \mu_{j-1})T_r} e^{A_c \tau} B_c d\tau \\ v_k \leq \mu_{(j-1)} : 0 \\ 0 = \mu_0 < \mu_1 < \dots < \mu_N = 1, \mu_j = j/N \\ 0 \leq v_1 < v_2 < \dots < \mu_N < 1, v_k = (k-1)/N \end{aligned} \quad (38)$$

Where equation B_l is a $a \ n \times n (= m \times N)$ square matrix since it has resulted from $B_j (j = 1, 2, \dots, N)$ that is a $m \times n$ matrix. Also, it is a regular matrix [16]. Thus, the input feedback

$$u_f(i) = [u_f(i, 1), \dots, u_f(i, N)]^T \quad (39)$$

And reference

$$y_r(i) = [y_r(i, 1), \dots, y_r(i, N)]^T \quad (40)$$

Results obtained from the state variable $\alpha_r(i+1) \in \mathbb{R}^n$ as follows:

$$u_f(i) = B_l^{-1}(I - z^{-1}A_l)\alpha_r(i+1) \quad (41)$$

$$y_r(i) = z^{-1}C_l \alpha_r(i+1) + D_l u_f(i) \quad (42)$$

Equation (41) is equivalent to the stable reverse system of the model. The system model can be expressed in two ways. The first model is the one that is derived directly from the physical model. But the second model is obtained from the MIMO controllable standard form. The control system for each of these models is illustrated in Figure (1).

The feedback control C_l has no limitation, but the controller's input can use only the errors of the link angle.

In this figure, another point, which considers the variable vector with subscript (i) as input and another type of vector with subscript (i, j) as output, is responsible for adding the vectors with different dimensions. However, we assume that the adder has a multirate holder function and a normal increasing function. Besides, we assume that the control reference is $r(i) = \alpha(i+1)$. Although many mechanical manipulators have angle sensors like rotary encoders on the servomotors, these sensors are not mounted directly on the links and connections.

In this paper, the state space model is used for observing the disturbance in order to estimate the joint angles directly. Figure (2) shows the block diagram of the observer and Figure (3) illustrates its structure.

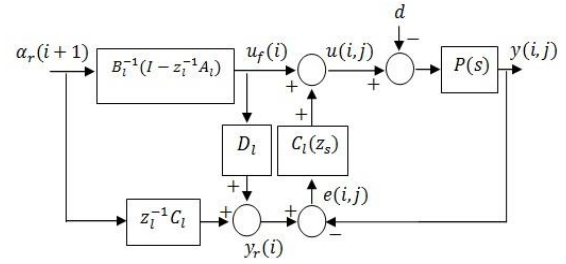


Fig. 1. Block diagram of the multirate control system 1

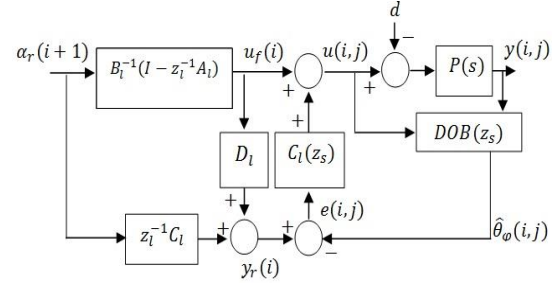


Fig. 2. Block diagram of the multirate control system 2

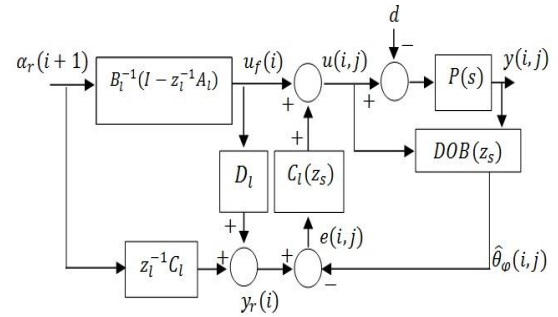


Fig. 3. Block diagram of disturbance observer

In the presented control system, the state variable vector $\alpha_r(i+1)$ is used with the delay of a sample as the reference $r(i)$. When designing the reference is done for a sample state variable vector, the feedforward section must be designed based on the model resulting from the physical model. Although it is not easy to directly determine the state variables for a complex system with low difficulty, a solution used for such cases is to use the controllable standard form.

The feature of this method is that the state variables z are related to their relevant time derivatives.

Although $C_c = \begin{bmatrix} 1 & 0 & 0 & 0 & 0 & 0 \\ 0 & 1 & 0 & 0 & 0 & 0 \end{bmatrix}$ is a matrix

for selecting two angles of the joints, $C = C_c S^{-1}$ at the output $y(t) = C_c S^{-1} z(t)$ of the standard form

doesn't deal with the selection of the special state variables, where the result is $z = [\alpha_1 \ \alpha_2 \ \dots \ \alpha_8]^T$.

On the contrary, when the output y is a state variable that indicates the link angles and is used as a reference for the control system, then the state variable z of the other joint angles will not represent the angular velocities or accelerations.

As for the presented system, the output equation for the controllable standard form can be expressed as a continuous system as follows:

$$\begin{bmatrix} \theta_{r1} \\ \theta_{r2} \end{bmatrix} = \begin{bmatrix} V_{11} & 0 & 0 & 0 & V_{12} & 0 & 0 & 0 \\ V_{21} & 0 & 0 & 0 & V_{22} & 0 & 0 & 0 \end{bmatrix} \begin{bmatrix} \alpha_1 & \alpha_2 & \dots & \alpha_8 \end{bmatrix}^T \quad (43)$$

This equation is rewritten as follows:

$$\begin{bmatrix} \theta_{r1} \\ \theta_{r2} \end{bmatrix} = \begin{bmatrix} V_{11} & V_{12} \\ V_{21} & V_{22} \end{bmatrix} \begin{bmatrix} \alpha_1 \\ \alpha_5 \end{bmatrix} \quad (44)$$

The coefficient matrix on the right side is a regular matrix.

Then, by defining

$$\begin{bmatrix} V_{11} & V_{12} \\ V_{21} & V_{22} \end{bmatrix}^{-1} = \begin{bmatrix} W_{11} & W_{12} \\ W_{21} & W_{22} \end{bmatrix} \quad (45)$$

And considering $\dot{\alpha}_1 = \alpha_2$, $\dot{\alpha}_2 = \alpha_3$, $\dot{\alpha}_3 = \alpha_4$, $\dot{\alpha}_5 = \alpha_6$, $\dot{\alpha}_6 = \alpha_7$, $\dot{\alpha}_7 = \alpha_8$ the state variables can be expressed using the joint angle variables through Equation (46).

$$\begin{bmatrix} \alpha_1 \\ \alpha_2 \\ \alpha_3 \\ \alpha_4 \\ \alpha_5 \\ \alpha_6 \\ \alpha_7 \\ \alpha_8 \end{bmatrix} = \begin{bmatrix} W_{11}I_4 & W_{12}I_4 \\ W_{21}I_4 & W_{22}I_4 \end{bmatrix} \begin{bmatrix} \theta_{r1} \\ \dot{\theta}_{r1} \\ \ddot{\theta}_{r1} \\ \theta_{r1}^{(3)} \\ \theta_{r2} \\ \dot{\theta}_{r2} \\ \ddot{\theta}_{r2} \\ \theta_{r2}^{(3)} \end{bmatrix} \quad (46)$$

The superscript (3) in θ_{r1}, θ_{r2} is indicative of the derivative of the 3rd order and can be used as the reference vector for the state vector $\alpha_r(i+1)$.

In addition, when the reference vector is specified, there will be two methods for determining the feedback section.

(Method-1): In this method, the reference vector of the state vector, which is expressed by Equation (45), is transformed into digital data using

the control ratio of T_1 . Then, the reference data is inserted as input into the feedforward, which is designed using the controllable standard form.

(Method-2): In this method, the reference vector of the state variable, which is expressed by Equation (46), is transformed to the variables of the previous state $X = S^{-1}Z$ and the variables are transformed into digital data by using the control ratio of T_1 . Finally, based on the physical model, the reference data are inserted as input into the feedforward section.



Fig. 4. Photograph of manipulator [18]

5. Simulations and Results

Considering the above-mentioned equations and formulas, first, we're going to introduce a set of initial equations and values that will be required for simulations.

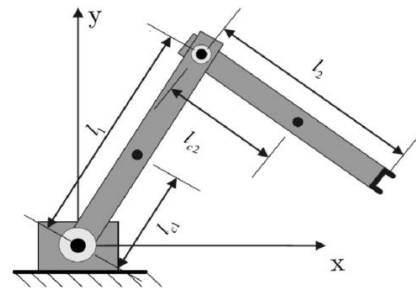


Fig. 5. Dynamic Model of manipulator Robot[20]

The robot considered for this work has got highly precise encoders at the outer side of the links. This means that the mechanical manipulator is equipped not only with rotary encoders connected to the self-adjusting engines but also with special rotary encoders. Figure (5) shows the image of the mechanical manipulator in which the black-coloured circular sections mounted on the joints are indeed the rotary encoders each with a precision of 1382400 pls/rot. The output of the engines and

harmonic decreasing gears are positioned behind the joints so they aren't visible in this figure.

Table.1.
Physical Parameters [10]-[11]

Symbol	Unit	Value	Symbol	Unit	Value
Mr1	Kgm2	2.21	Dm1	Nms/rad	15.88
Mr2	Kgm2	0.42	Dm2	Nms/rad	6.52
Dr1	Nms/rad	15.88	DmC1	Nm	9.53
Dr2	Nms/rad	6.52	DmC2	Nm	8.48
DrC1	Nm	18.39	kn1	Nm/rad	10000
DrC2	Nm	8.66	kn2	Nm/rad	3000
R	Kgm2	0.2	dn1	Nm/rad	15.88
Im1	Kgm2	2.45E-4	dn2	Nm/rad	6.52
Im2	Kgm2	7.62E-5	n1,n2	(No-dim.)	161,121
Resm	Pls/rev	8,196	Resj	Pls/rev	1,382,400

Table.2.
Control Parameters

Name	Value
Sampling time Ts 2 (ms)	
Sampling time Ts 8 (ms)	
Poles of 1st OB	[0.68,0.69,0.70,0.71,0.72,0.73,0.74,0.75]
Q	diag(104,104,104,1,1,1,1,5×108, 5×107)
R	diag(102,102)

The simulation results are presented in this section. Table (2) presents the parameters applied to these simulations. The results of the simulation while using of the multirate feedforward control are given in Figure (6). And Figure (7) shows the results obtained without using the multirate feedforward control. Both controls utilize state space disturbance observers for estimating the joint angles.

In such cases, the highly precise rotary encoders are used only for the assessment of precision (accuracy). Figure (8) shows the simulation results while using the multirate feedforward control wherein the data's direct feedback from the highly precise rotary encoders has been used.

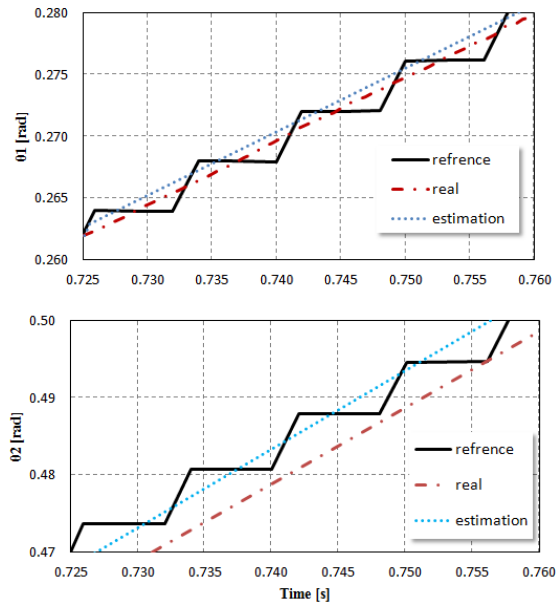
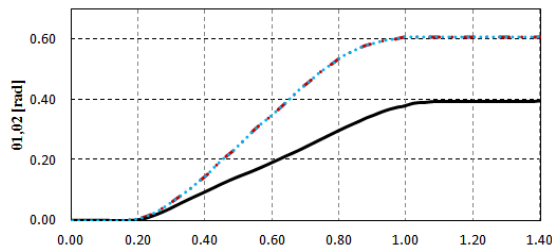


Fig. 6. Simulation results while using the multirate feedforward control and estimation of joint angles

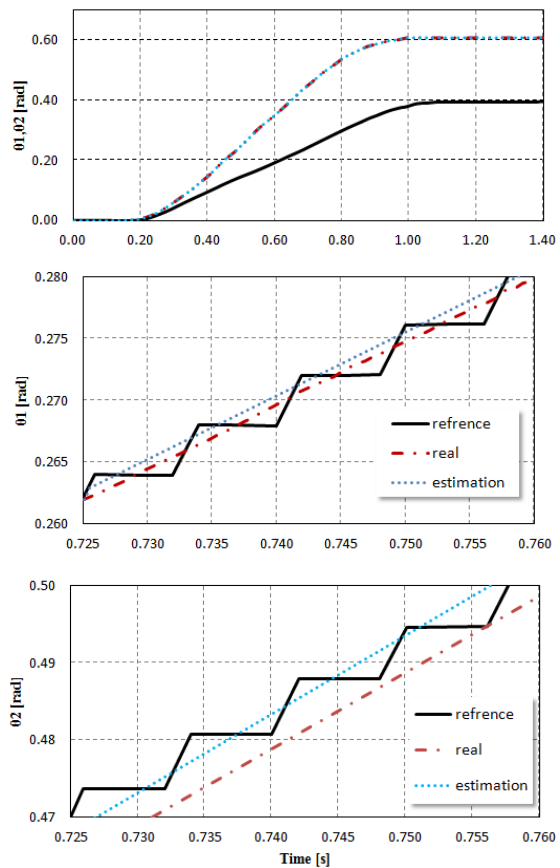


Fig. 7. Simulation experimental results obtained without feedforward control and joint angles estimation

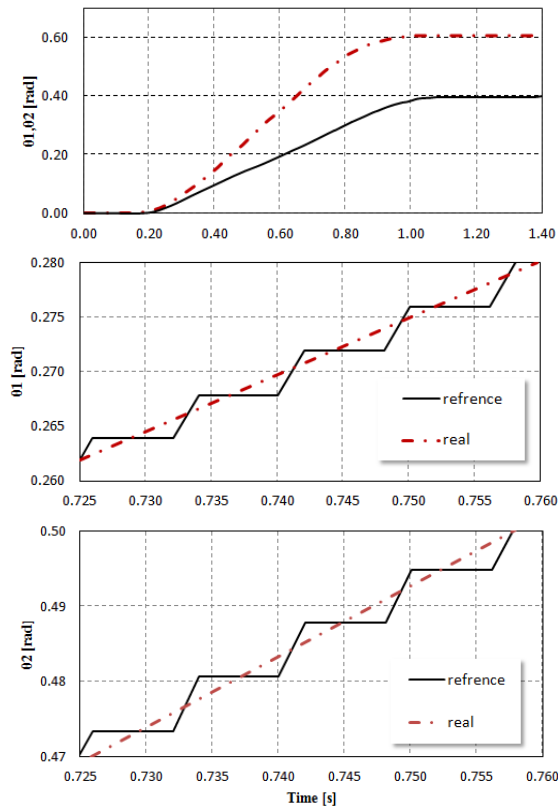


Fig. 8. Experimental results obtained from feedforward and rotary encoding with high

From Comparing Figures (5) and (6) shows that the waveforms of the estimates of the joint angles are in accordance with the reference angles.

Accordingly, the use of the multirate feedforward controlled to better results than the case without it. In addition, there are small errors and differences between the estimations and real data, which seem to be due to the slight parameter errors in the physical model of the manipulator.

Figure (8) shows the very good tracking performance of the real joint angles. This indicates that the use of the proposed control law and encoder would lead to Good performance of the mechanical manipulators. The control signal and tracking error diagram components are shown in Figures (9) and (10), respectively, which converge to zero over an acceptable period of time.

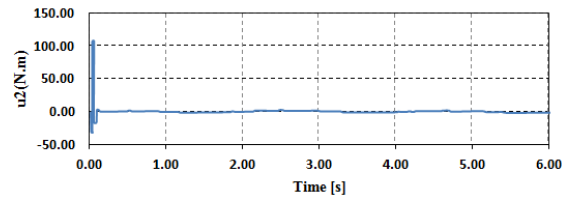
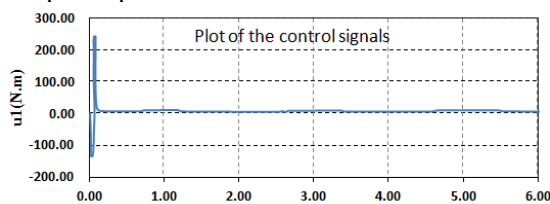


Fig. 9. The 1st and 2nd components of the control signal

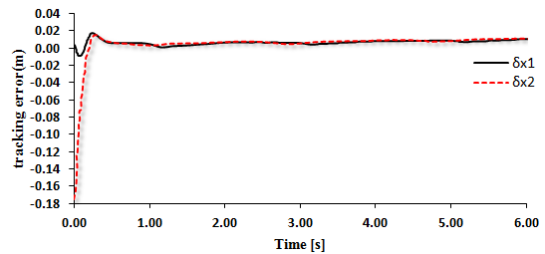


Fig. 10. Tracking error signal

6. Conclusion

The present paper introduces a practical method for designing and executing the multirate feedforward control of robotic mechanical manipulator. First, to eliminate the effect of disturbance, a passivity-based control was designed and it was shown that it, unlike the reverse dynamic control, didn't require linearization.

Considering the significant effect of the sampling rate on the examination of stability and tracking of the practical systems, the control structure was defined in a multirate form. Such a multirate structure allows the designer to be free in making decisions on the sampling time as one of the control parameters and increase or decrease it depending on the robotic manipulator's motion path.

The simulation results for this control as well as its effect on the estimation of the angles of the joints indicated the high-precision tracking compared to the continuous or single-rate controls.

The process of designing a control is a systematic process and also simple in terms of implementation. Therefore, it is expected that this technology can be used for regular robotic manipulators and is associated with promising outcomes in the future. The main idea used in this paper, compared to the previous works, is the use of the multirate control and the consideration of the sampling time as one of the control parameters. This enables the designer to make decision on the time and increase or decrease it depending on the robot's motion path. The simulations performed in this study indicate the precision of the estimation of the joint angles in comparison with the single-rate control for this state.

References

- [1] G. Gu and L. Qiu, "Networked stabilization of multi-input systems with channel resource allocation," in Proceedings of the 17th IFAC World Congress, 2008, pp. 625-630.
- [2] R. Wang, "The interplay between the awareness-based resource allocation and epidemic spreading on multiplex networks," in 2021 IEEE 5th Advanced Information Technology, Electronic and Automation Control Conference (IAEAC), 2021, pp. 583-586.
- [3] W. Chen, J. Zheng, and L. Qiu, "Linear quadratic optimal control of continuous-time LTI systems with random input gains," in Information and Automation (ICIA), 2012 International Conference on, 2012, pp. 241-246.
- [4] W. Guan, H. Zhang, and V. C. Leung, "Analysis of Traffic Performance on Network Slicing Using Complex Network Theory," IEEE Transactions on Vehicular Technology, 2020.
- [5] J. Zheng, W. Chen, L. Shi, and L. Qiu, "Linear quadratic optimal control for discrete-time LTI systems with random input gains," in Control Conference (CCC), 2012 31st Chinese, 2012, pp. 5803-5808.
- [6] A. N. Serov, D. A. Chumachenko, and A. A. Shatokhin, "Application of Random Functions to Assess the Influence of Quantization Error on the Signal RMS," in 2020 Ural Smart Energy Conference (USEC), 2020, pp. 43-46.
- [7] X. Yang, C. Hua, J. Yan, and X. Guan, "New stability criteria for networked teleoperation system," Information Sciences, vol. 233, pp. 244-254, 2013.
- [8] M. Steinberger and M. Horn, "A Stability Criterion for Networked Control Systems With Packetized Transmissions," IEEE Control Systems Letters, vol. 5, pp. 911-916, 2020.
- [9] M. Cloosterman, N. van de Wouw, M. Heemels, and H. Nijmeijer, "Robust stability of networked control systems with time-varying network-induced delays," in Decision and Control, 2006 45th IEEE Conference on, 2006, pp. 4980-4985.
- [10] C. Tan, H. Zhang, W. S. Wong, and Z. Zhang, "Feedback Stabilization of Uncertain Networked Control Systems over Delayed and Fading Channels," IEEE Transactions on Control of Network Systems, 2020.
- [11] P. Naghshtabrizi, J. P. Hespanha, and A. R. Teel, "Stability of delay impulsive systems with application to networked control systems," Transactions of the Institute of Measurement and Control, vol. 32, pp. 511-528, 2010.
- [12] H. Li, Y. Fan, G. Pan, and C. Song, "Event-Triggered Remote Dynamic Control for Network Control Systems," in 2020 16th International Conference on Control, Automation, Robotics and Vision (ICARCV), 2020, pp. 483-488.
- [13] K. Liu and E. Fridman, "Networked-based stabilization via discontinuous Lyapunov functionals," International Journal of Robust and Nonlinear Control, vol. 22, pp. 420-436, 2012.
- [14] M. Bahraini, M. Zanon, A. Colombo, and P. Falcone, "Optimal Control Design for Perturbed Constrained Networked Control Systems," IEEE Control Systems Letters, vol. 5, pp. 553-558, 2020.
- [15] M. Moarref and L. Rodrigues, "On exponential stability of linear networked control systems," International Journal of Robust and Nonlinear Control, vol. 24, pp. 1221-1240, 2014.
- [16] Y. Kosaka and A. Shimada, "Motion control for articulated robots based on accurate modeling," in The 8th IEEE International Workshop on Advanced Motion Control, 2004. AMC'04., 2004, pp. 535-540.
- [17] Rosolia U, Ames AD. Multi-rate control design leveraging control barrier functions and model predictive control policies. IEEE Control Systems Letters. 2020 Jul 9;5(3):1007-12.
- [18] Chen WH, He H, Lu X. Multi-rate sampled-data composite control of linear singularly perturbed systems. Journal of the Franklin Institute. 2020 Mar 1;357(4):2028-48.
- [19] Li Z, Xue SR, Yu XH, Gao HJ. Controller optimization for multirate systems based on reinforcement learning. International Journal of Automation and Computing. 2020 Jun;17(3):417-27.
- [20] Ghiassi AR, Ghavifekr AA, Hagh YS, SeyedGholami H. Designing adaptive robust extended Kalman filter based on Lyapunov-based controller for robotics manipulators. In 2015 6th International Conference on Modeling, Simulation, and Applied Optimization (ICMSAO) 2015 May 27 (pp. 1-6). IEEE.